



# VIBRATION ANALYSIS OF A TIMOSHENKO BEAM SUBJECTED TO A TRAVELLING MASS

E. ESMAILZADEH AND M. GHORASHI

*Department of Mechanical Engineering, Sharif University of Technology, Tehran, Iran*

*(Received 19 July 1995, and in final form 3 May 1996)*

The analysis of the Timoshenko beam traversed by uniform partially distributed moving masses is carried out. Equations of motion are solved by using a finite difference based algorithm. The beam response, and the distribution of the shear force and bending moment along the beam have been computed. The effects of shear deformation, rotary inertia and the length of load distribution on the vibration of the beam have been analyzed. The results compare well with those reported in the literature for the limiting case in which the length of the load distribution reduces to zero and also the effects of shear deformation and rotary inertia are neglected.

© 1997 Academic Press Limited

## 1. INTRODUCTION

A moving load produces larger beam deflections and stresses than when the same load acts statically. Hence the analysis of structures carrying such loadings is of considerable practical importance. Investigation of bridges on which heavy vehicles travel, and trolleys of overhead travelling cranes moving on their girders, are two examples of such dynamical systems.

Since the middle of the last century, when railway construction began, the problem of oscillation of bridges under travelling loads has interested many engineers [1]. Timoshenko [2] considered the case of a pulsating load passing over a bridge, while Inglis [3] performed an analysis of trains crossing a bridge, and considered many important factors such as the effect of the moving load, the influences of damping and suspension of locomotives.

The case of a concentrated force moving with a constant velocity along a beam, when neglecting damping forces, was solved by Timoshenko [4] and an expression for the critical velocity was presented. The dynamic analysis of a simply supported beam carrying a moving mass was carried out by Stanisic and Hardin [5]; this is interesting enough in itself, but not easily applicable to different boundary conditions. Two prominent publications concerning the behavior of a beam carrying a moving concentrated mass under different situations are those of Leech [6] and Cifuentes [7].

A comprehensive treatment of the subject for the vibration of structures resulting from moving loads, which contains a large number of related cases, has been given by Frýba [8]. Ghorashi [9–11] has investigated many cases of moving load problems. The vibration of an Euler–Bernoulli beam traversed by uniform partially distributed moving mass has also been studied [12]. A further investigation has been made by Lin [13], which he has discussed with the authors. The authors' response to his comments is given in the Appendix.

The present work extends the scope of the previous study [12] by considering the vibration of a Timoshenko beam when subjected to a uniform partially distributed moving

mass. Evidently, the model considered for the moving mass may be appropriate in cases in which the length of the load distribution is not negligible. Furthermore, since no point mass exists physically, consideration of an interval for the load distribution enhances the reality of the problem formulation. The point mass formulation can be considered as a special case of the present problem if the load distribution interval is assumed to be small [10]. Therefore, the degree of influence of parameters such as the length of the load distribution, rotary inertia and shear deformation could also be evaluated.

In the present work, the following assumptions are adopted. First, the beam is assumed to be of constant cross-section with uniform mass distribution: furthermore, its dynamic characteristics are described by the Timoshenko beam equations. Second, the effects of inertia for both the beam and the moving mass are taken into account with the gravitational effect of load. Third, the load moves with a uniform speed and is guided in such a way that it keeps contact with the beam at all times. Fourth, the computations are performed for simply supported boundary conditions. Finally, as to the initial conditions, the beam is assumed to be free of either the load or the deflections.

## 2. EQUATIONS OF MOTION

With reference to Figure 1, it is assumed that, at  $t = 0$ , the load is starting to enter the beam from the left-hand support, at a constant speed  $V$ . The reference state of the beam is its equilibrium position under its own weight. Hence, at  $t = 0$ , all initial conditions of the beam are zero. The mass  $M_p$  is assumed to be uniformly distributed over a fixed length  $\varepsilon$  of the beam. The beam is assumed to be simply supported at both ends. However, the analysis and formulation presented are not limited to just these boundary conditions.

In respect to the effects of shear deformation, the following constitutive equations hold;

$$EI \partial\psi/\partial x = M, \quad \psi - \partial y/\partial x = S/kAG. \quad (1, 2)$$

Here  $E$  is the Young's modulus of elasticity,  $A$  is the constant cross-sectional area of the beam,  $G$  is the shear modulus,  $S$  is the beam shear force,  $M$  is the bending moment,  $\psi$  is the slope of the beam due to the bending and  $k$  is the shear coefficient, which depends on the shape of the beam cross-section.

Furthermore, in respect to the effect of rotary inertia of the beam and that of the moving mass, the two equations of motion for an element of the beam are

$$\frac{\partial S}{\partial x} + \rho A \frac{\partial^2 y}{\partial t^2} + \frac{1}{\varepsilon} \left[ M_p g + M_p \frac{d^2 y}{dt^2} \right] D = 0, \quad S - \frac{\partial M}{\partial x} + \rho I \frac{\partial^2 \psi}{\partial t^2} + \rho_p I_p \frac{d^2 \psi}{dt^2} D = 0, \quad (3, 4)$$

where  $\rho$  and  $\rho_p$  are the respective mass densities of the beam and the load, while  $I$  and  $I_p$  denote the corresponding moments of their cross-sectional area, respectively. In writing the equations of motion, it has been assumed that the load is quite flexible and is spread along the beam with no possibility of separation. Therefore, values of shearing force and bending moment in the load have been neglected in comparison with their corresponding values for the beam. If the load is able to bear shearing forces and bending moments, it can no longer be assumed that the deflections and slopes in the beam and corresponding points of the mass are identical. Hence the "no separation" assumption would be violated.

The factor  $D$  depends on the interval of motion, which is the part of the beam supporting the moving mass:

$$D = \begin{cases} 1 - H(x - \xi - \epsilon/2), & 0 \leq t < \epsilon/V, \\ H(x - \xi + \epsilon/2) - H(x - \xi - \epsilon/2), & \epsilon/V \leq t < L/V, \\ H(x - \xi + \epsilon/2), & L/V \leq t < (L + \epsilon)/V, \\ 0, & (L + \epsilon)/V \leq t, \end{cases} \quad (5)$$

where  $\xi = Vt - \epsilon/2$  is as shown in Figure 1, and  $H(x)$  is defined as

$$H(x) = \begin{cases} 1, & x > 0, \\ 0.5, & x = 0, \\ 0, & x < 0. \end{cases} \quad (6)$$

The dynamic part of the moving load acceleration in equation (3) is expected to dominate the gravitational acceleration, when the load is travelling at high velocities.

For the total derivatives in equations (3) and (4) one may write

$$\frac{d^2y}{dt^2} = \frac{\partial^2y}{\partial t^2} + 2V \frac{\partial^2y}{\partial x \partial t} + V^2 \frac{\partial^2y}{\partial x^2}, \quad \frac{d^2\psi}{dt^2} = \frac{\partial^2\psi}{\partial t^2} + 2V \frac{\partial^2\psi}{\partial x \partial t} + V^2 \frac{\partial^2\psi}{\partial x^2}. \quad (7, 8)$$

In view of equations (1) and (2), equations (7) and (8) reduce to,

$$\frac{d^2y}{dt^2} = \frac{\partial^2y}{\partial t^2} + V \frac{\partial^2y}{\partial t \partial x} - \frac{V}{kAG} \left[ \frac{\partial S}{\partial t} + V \frac{\partial S}{\partial x} \right] + V \left[ \frac{\partial \psi}{\partial t} + V \frac{M}{EI} \right], \quad (9)$$

$$\frac{d^2\psi}{dt^2} = \frac{\partial^2\psi}{\partial t^2} + V \frac{\partial^2\psi}{\partial x \partial t} + \frac{V}{EI} \left[ \frac{\partial M}{\partial t} + V \frac{\partial M}{\partial x} \right]. \quad (10)$$

Substituting equations (9) and (10) into equations (3) and (4), with  $\partial y/\partial t$  and  $\partial \psi/\partial t$  denoted by  $z$  and  $Q$ , respectively, yields

$$\left[ g + \frac{\partial z}{\partial t} + V \frac{\partial z}{\partial x} - \frac{V}{kAG} \left[ \frac{\partial S}{\partial t} + V \frac{\partial S}{\partial x} \right] + V \left[ Q + V \frac{M}{EI} \right] \right] \frac{M_p D}{\epsilon} + \frac{\partial S}{\partial x} + \rho A \frac{\partial z}{\partial t} = 0, \quad (11)$$

$$\rho_p I_p \left[ \frac{\partial Q}{\partial t} + V \frac{\partial Q}{\partial x} + \frac{V}{EI} \left[ \frac{\partial M}{\partial t} + V \frac{\partial M}{\partial x} \right] \right] D + S - \frac{\partial M}{\partial x} + \rho I \frac{\partial Q}{\partial t} = 0. \quad (12)$$

Similarly, for equations (1) and (2), one obtains

$$\partial M/\partial t = EI \partial Q/\partial x, \quad \partial S/\partial t = kAG[Q - \partial z/\partial x]. \quad (13, 14)$$

The four first order partial differential equations (11)–(14) can now be solved numerically for the four dependent variables  $M$ ,  $S$ ,  $Q$  and  $z$ .

In order to derive the final equations in a more general form, and suitable for performing numerical calculations with reduced computational errors, it is appropriate to convert the equations into equivalent non-dimensional ones. The characteristic variables for the current problem may be considered as the following:  $L$ , characteristic length;  $K = \sqrt{I/A}$ , characteristic deflection;  $K/L = \lambda$ , characteristic rotation;  $\lambda c$ , characteristic velocity ( $c = \sqrt{E/\rho}$ );  $L/\lambda c$ , characteristic time;  $\rho AL$ , characteristic mass. Hence, the non-dimensional variables are

$$y_n = y/K, \quad \psi_n = \psi/\lambda, \quad x_n = x/L, \quad t_n = \lambda c t/L, \\ M_{pn} = M_p/\rho AL, \quad V_n = V/\lambda c, \quad \epsilon_n = \epsilon/L.$$

The non-dimensional shear force and bending moment may now be defined as

$$M_n = \partial\psi/\partial x_n, \quad S_n = \psi_n - \partial y_n/\partial x_n. \quad (15, 16)$$

Therefore, by considering equations (1) and (2), one obtains

$$M_n = (L^2/EIK)M, \quad S_n = S/kAG\lambda. \quad (17, 18)$$

Similarly, for  $Q_n$  and  $z_n$ , defined as

$$Q_n = \partial\psi_n/\partial t_n, \quad z_n = \partial y_n/\partial t_n, \quad (19, 20)$$

it can be seen that, by using the definitions for  $Q$  and  $z$ ,

$$Q_n = (L/\lambda^2 c)Q, \quad z_n = (L/K\lambda c)z. \quad (21, 22)$$

Hence, equations (11)–(14) can be transformed to the following non-dimensional forms;

$$\left[ g_n + \frac{\partial z_n}{\partial t_n} + V_n \frac{\partial z_n}{\partial x_n} - V_n \left[ \frac{\partial S_n}{\partial t_n} + V_n \frac{\partial S_n}{\partial x_n} \right] + V_n [Q_n + V_n M_n] \right] \left( \frac{M_{pn} D}{\epsilon_n} \right) + \frac{\partial z_n}{\partial t_n} + \alpha \frac{\partial S_n}{\partial x_n} = 0, \quad (23)$$

$$R\lambda^2 \left[ \frac{\partial Q_n}{\partial t_n} + V_n \frac{\partial Q_n}{\partial x_n} + V_n \left[ \frac{\partial M_n}{\partial t_n} + V_n \frac{\partial M_n}{\partial x_n} \right] \right] D - \frac{\partial M_n}{\partial x_n} + \alpha S_n + \lambda^2 \frac{\partial Q_n}{\partial t_n} = 0, \quad (24)$$

$$\partial M_n/\partial t_n = \partial Q_n/\partial x_n, \quad \partial S_n/\partial t_n = Q_n - \partial z_n/\partial x_n. \quad (25, 26)$$

Here,  $\alpha = kG/E\lambda^2$ ,  $R = \rho_p I_p/\rho I$  and  $g_n = (L/\lambda^3 c^2)g$ .

### 3. FINITE DIFFERENCE FORMULATION

The set of four first order partial differential equations (23)–(26) need to be solved for  $M_n$ ,  $S_n$ ,  $Q_n$  and  $z_n$ . To this end, these differential equations may be transformed into equivalent algebraic finite difference ones.

Assuming  $\phi(x, t)$  to be any of the dependent variables, and that, at beam node  $i$ ,  $\phi_i = \phi(x, t)$ , then at points neighboring  $(x, t)$ ,  $\phi$  may be represented as

$$\phi_{i+1} = \phi(x + \Delta x, t), \quad \phi_i^+ = \phi(x, t + \Delta t), \quad \phi_{i+1}^+ = \phi(x + \Delta x, t + \Delta t). \quad (27)$$

Then, using a four-point difference scheme yields

$$\phi(x + \Delta x/2, t + \Delta t/2) = \frac{1}{4}[\phi_{i+1}^+ + \phi_{i+1} + \phi_i^+ + \phi_i] + O[\Delta x^2, \Delta t^2], \quad (28)$$

which states that the function value at the center of an  $x$ – $t$  grid may be well approximated by the average of its values at the grid nodes.

Similarly, by using the definition of partial derivatives,

$$\frac{\partial \phi}{\partial t} \left( x + \frac{\Delta x}{2}, t + \frac{\Delta t}{2} \right) = \frac{1}{2\Delta t} [\phi_{i+1}^+ + \phi_i^+ - \phi_{i+1} - \phi_i] + O[\Delta x^2, \Delta t^2], \quad (29)$$

$$\frac{\partial \phi}{\partial x} \left( x + \frac{\Delta x}{2}, t + \frac{\Delta t}{2} \right) = \frac{1}{2\Delta x} [\phi_{i+1}^+ + \phi_{i+1} - \phi_i^+ - \phi_i] + O[\Delta x^2, \Delta t^2], \quad (30)$$

Furthermore, since the term  $\partial\phi/\partial t + V\partial\phi/\partial x$  has been generated in the final form of the governing equations, it is appropriate to find its corresponding finite difference

representation. Using equations (29) and (30), and assuming  $\Delta x/\Delta t = V$ , i.e., at each time interval one space interval is travelled by the moving mass, one obtains

$$\left(\frac{\partial}{\partial t} + V\frac{\partial}{\partial x}\right)\phi\left(x + \frac{\Delta x}{2}, t + \frac{\Delta t}{2}\right) = \frac{1}{\Delta t}(\phi_{i+1}^+ - \phi_i) \tag{31}$$

Equations (28)–(31) are considered to be the governing equations of the current problem; i.e., equations (23)–(26) may be transformed into equivalent finite difference equations. For this purpose the non-dimensional space and time increments may be defined as  $\Delta x_n = \Delta x/L$  and  $\Delta t_n = \lambda c\Delta t/L$ . Transforming the non-dimensional variables in equations (23)–(26) into their corresponding dimensional ones for simplicity, one obtains

$$M_{i+1}^+ + M_i^+ - (1/V)(Q_{i+1}^+ - Q_i^+) = M_{i+1} + M_i + (1/V)(Q_{i+1} - Q_i) = \Delta_i^1, \tag{32}$$

$$\begin{aligned} S_{i+1}^+ + S_i^+ + \frac{1}{V}(z_{i+1}^+ - z_i^+) - \frac{\Delta t}{2}(Q_{i+1}^+ + Q_i^+) \\ = S_{i+1} + S_i - \frac{1}{V}(z_{i+1} - z_i) + \frac{\Delta t}{2}(Q_{i+1} + Q_i) = \Delta_i^2, \end{aligned} \tag{33}$$

$$\begin{aligned} M_{i+1}^+ - M_i^+ - (\alpha\Delta x/2)(S_{i+1}^+ + S_i^+) - \lambda^2 V(Q_{i+1}^+ + Q_i^+) - 2RV\lambda^2 Q_{i+1}^+ D - 2RV\lambda^2 M_{i+1}^+ D \\ = -M_{i+1} + M_i + (\alpha\Delta x/2)(S_{i+1} + S_i) - \lambda^2 V(Q_{i+1} + Q_i) - 2R\lambda^2 VQ_i D - 2R\lambda^2 V^2 M_i D \\ = \Delta_i^3, \end{aligned} \tag{34}$$

and

$$\begin{aligned} S_{i+1}^+ - S_i^+ + (V/\alpha)(z_{i+1}^+ + z_i^+) + (2M_p\Delta x/\alpha\varepsilon)[(1/\Delta t)z_{i+1}^+ - (V/\Delta t)S_{i+1}^+ \\ + (V/4)(Q_{i+1}^+ + Q_i^+) + (V^2/4)(M_{i+1}^+ + M_i^+)]D \\ = -(S_{i+1} - S_i) + (V/\alpha)(z_{i+1} + z_i) - (2M_p\Delta x/\alpha\varepsilon)[g - (1/\Delta t)z_i + (V/\Delta t)S_i \\ + (V/4)(Q_{i+1} + Q_i) + (V^2/4)(M_{i+1} + M_i)]D = \Delta_i^4. \end{aligned} \tag{35}$$

Equations (32)–(35) may be expressed as the matrix

$$\begin{aligned} &\begin{bmatrix} 1 & 0 & 1/V & 0 \\ 0 & 1 & -\Delta t/2 & -1/V \\ -1 & -\alpha\Delta x/2 & -\lambda^2 V & 0 \\ M_p V^2 D/2\alpha\gamma & -1 & M_p V D/2\alpha\gamma & V/\alpha \end{bmatrix} \begin{bmatrix} M_i^+ \\ S_i^+ \\ Q_i^+ \\ z_i^+ \end{bmatrix} \\ &+ \begin{bmatrix} 1 & 0 & -1/V & 0 \\ 0 & 1 & -\Delta t/2 & 1/V \\ 1 - 2R\lambda^2 V^2 D & -\alpha\Delta x/2 & -\lambda^2 V - 2R\lambda^2 V D & 0 \\ M_p V^2 D/2\alpha\gamma & 1 - 2M_p V^2 D/\alpha\varepsilon & M_p \Delta x V D/2\alpha\varepsilon & V/\alpha + 2M_p \Delta x D/\alpha\varepsilon \Delta t \end{bmatrix} \\ &\times \begin{bmatrix} M_{i+1}^+ \\ S_{i+1}^+ \\ Q_{i+1}^+ \\ z_{i+1}^+ \end{bmatrix} = \begin{bmatrix} \Delta_i^1 \\ \Delta_i^2 \\ \Delta_i^3 \\ \Delta_i^4 \end{bmatrix}, \end{aligned} \tag{36}$$

where,  $\gamma = \varepsilon/\Delta x$  is an integer. Upon introducing,

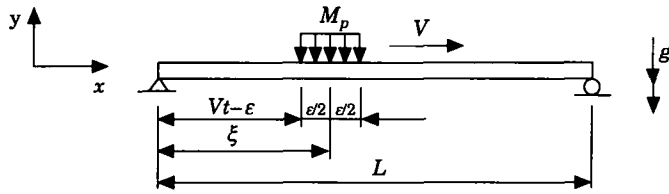


Figure 1. The model of the problem.

$$q_i = \begin{bmatrix} M_i^+ \\ S_i^+ \\ Q_i^+ \\ z_i^+ \end{bmatrix}, \quad q_{i+1} = \begin{bmatrix} M_{i+1}^+ \\ S_{i+1}^+ \\ Q_{i+1}^+ \\ z_{i+1}^+ \end{bmatrix}, \quad E_i = \begin{bmatrix} \Delta_i^1 \\ \Delta_i^2 \\ \Delta_i^3 \\ \Delta_i^4 \end{bmatrix}$$

the set of algebraic equations to be solved, can be written as

$$C_i q_i + D_i q_{i+1} = E_i, \quad \text{for } i = 1, 2, \dots, N - 1, \tag{37}$$

where  $N$  is the number of the nodal points dividing the beam.

Clearly, if only one of the above equations is used, by having the data at a specific time step, the calculation of parameters at the next time step reduces to the solution of four equations with eight unknowns. As will be shown later, the application of boundary conditions reduces this to a set of four equations with four unknowns.

#### 4. EULER-BERNOULLI BEAM

Before proceeding, it is suitable to simplify the results obtained to those for the case of an Euler-Bernoulli beam, where the effects of shear deformation and rotary inertia can be assumed to be negligible. This not only enables one to evaluate the influence of these factors, but also results in a new formulation for analyzing Euler-Bernoulli beam response when subjected to dynamic forces due to the motion of a uniform partially distributed mass. It may be recalled that Esmailzadeh and Ghorashi [12] have presented a formulation for the case of an Euler-Bernoulli beam using a completely different approach.

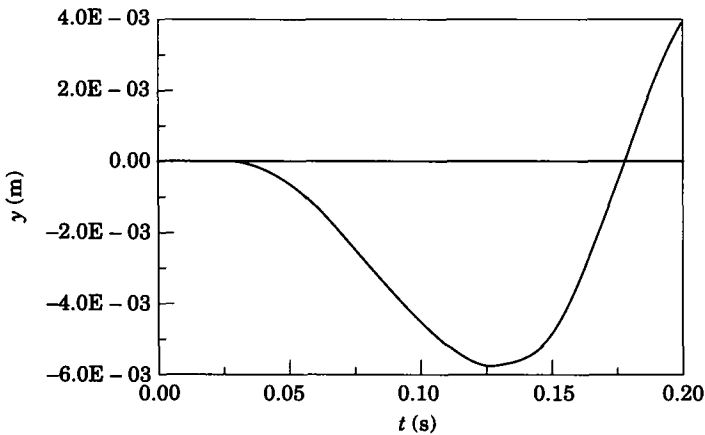


Figure 2. The time history diagram of the center of the beam.

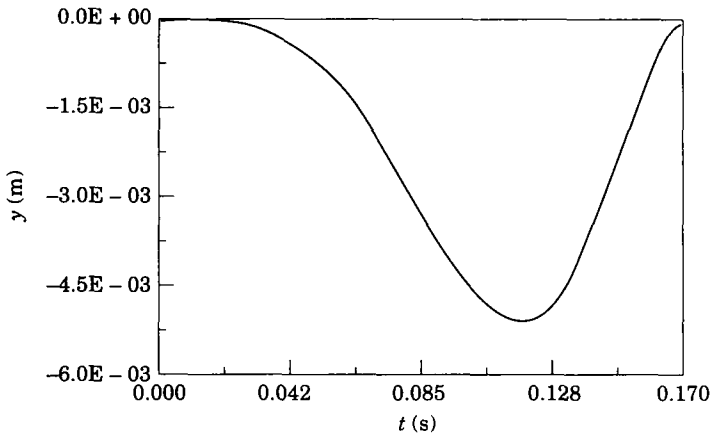


Figure 3. The trajectory of motion for the moving mass center.

Comparison of the results obtained from these two different algorithms, for the case under consideration, may be implemented for evaluation of solution accuracy.

4.1. NO SHEAR DEFORMATION (RAYLEIGH BEAM)

In this case,  $\psi = \partial y / \partial x$  and hence in consideration of equation (2) the value of the shear coefficient should be made very large (mathematically, infinite). However, consideration of very large values for this parameter results in some difficulties, especially regarding  $S_n$ . Therefore, instead of presenting a new formulation with the shear coefficient taken to be infinite, one may use the previous results with a sufficiently large value for the shear coefficient. The only problem will then be the addition of some computational error in the results. Fortunately, an estimation for this error can simply be obtained. From equation (2), the following expression may be written for the percentage of error when assuming the shear coefficient not to be infinite (a central difference equivalent for the left side has been written):

$$100 \frac{S/kAG}{\partial y / \partial x} \approx \frac{200S_i \Delta x}{kAG(y_{i+1} - y_{i-1})} \tag{38}$$

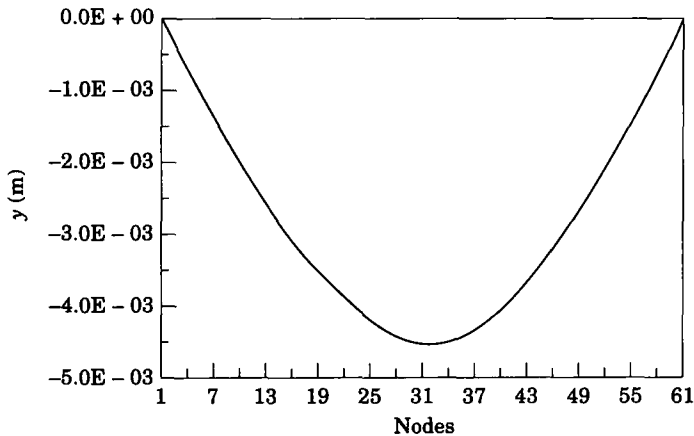


Figure 4. The beam deflected shape at  $t = 0.1$  s.

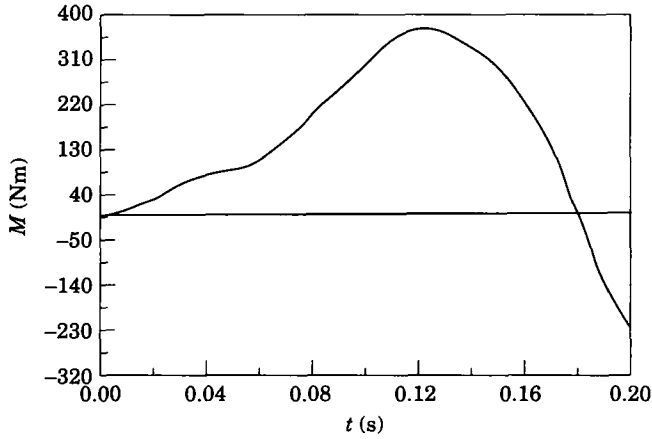


Figure 5. The maximum bending moment variation (positive or negative).

Since all the parameters in equation (38) are computed during the solution, the error percentage can be calculated at each time step. If this error is more than the acceptable value, then it is only necessary to increase the shear coefficient so that the error lies in the acceptable bound. Therefore one may be sure that the shear deformation effect has been limited to the feasible amount.

4.2. NO ROTARY INERTIA (SHEAR BEAM)

In order to obtain the formulation when neglecting the rotary inertia effect, it is only necessary to rewrite equation (4), dropping the term associated with the beam rotary inertia. Hence

$$S - \partial M / \partial x + \rho_p I_p (d^2 \psi / dt^2) D = 0, \tag{39}$$

Therefore equation (34) reduces to

$$\begin{aligned} M_{i+1}^+ - M_i^+ - (\alpha \Delta x / 2) (S_{i+1}^+ + S_i^+) - 2RV\lambda^2 Q_{i+1}^+ D - 2RV^2 \lambda^2 M_{i+1}^+ D \\ = -M_{i+1} + M_i + (\alpha \Delta x / 2) (S_{i+1} + S_i) - 2R\lambda^2 V Q_i D - 2R\lambda^2 V^2 M_i D \\ = \Delta_i^3. \end{aligned} \tag{40}$$

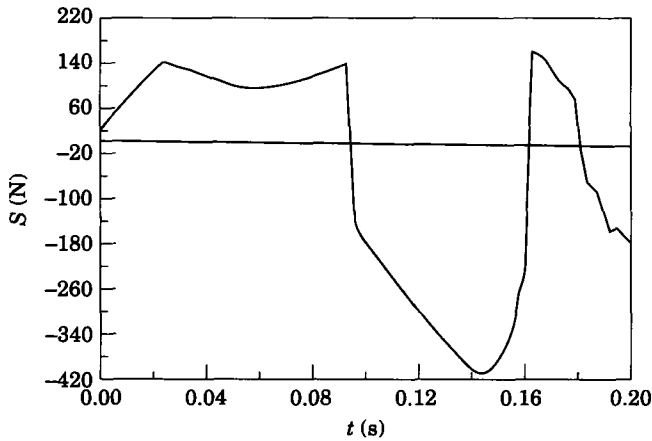


Figure 6. The maximum shear force variation (positive or negative).



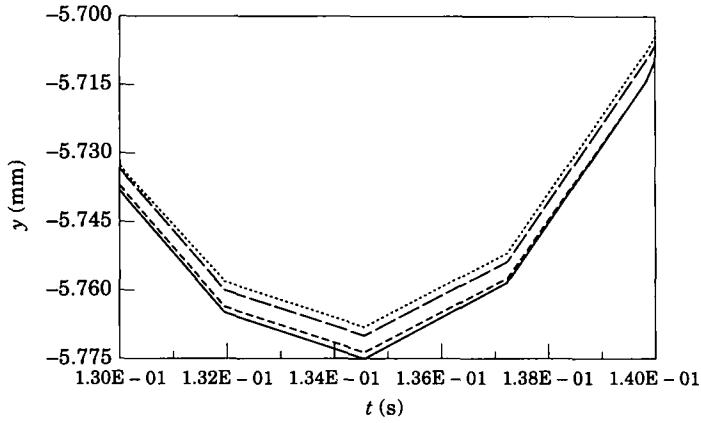


Figure 7. Part of the time history diagram at the center, for thin beam data. —, Timoshenko; ----, no rotary inertia; - · - ·, no shear deformation; · · · ·, Euler-Bernoulli.

Finally, equation (36) is transformed to

$$\begin{aligned}
 & \begin{bmatrix} 1 & 0 & 1/V & 0 \\ 0 & 1 & -\Delta t/2 & -1/V \\ -1 & -\alpha \Delta x/2 & 0 & 0 \\ M_p V^2 D/2\alpha\gamma & -1 & M_p V D/2\alpha\gamma & V/\alpha \end{bmatrix} \begin{bmatrix} M_i^+ \\ S_i^+ \\ Q_i^+ \\ z_i^+ \end{bmatrix} \\
 & + \begin{bmatrix} 1 & 0 & -1/V & 0 \\ 0 & 1 & -\Delta t/2 & 1/V \\ 1 - 2R\lambda^2 V^2 D & -\alpha \Delta x/2 & -2R\lambda^2 V D & 0 \\ M_p V^2 D/2\alpha\gamma & 1 - 2M_p V^2 D/\alpha\epsilon & M_p \Delta x V D/2\alpha\epsilon & V/\alpha + 2M_p \Delta x D/\alpha\epsilon \Delta t \end{bmatrix} \\
 & \times \begin{bmatrix} M_{i+1}^+ \\ S_{i+1}^+ \\ Q_{i+1}^+ \\ z_{i+1}^+ \end{bmatrix} = \begin{bmatrix} \Delta_i^1 \\ \Delta_i^2 \\ \Delta_i^3 \\ \Delta_i^4 \end{bmatrix} \quad (41)
 \end{aligned}$$

Hence, the formulation when neglecting rotary inertia is obtained.

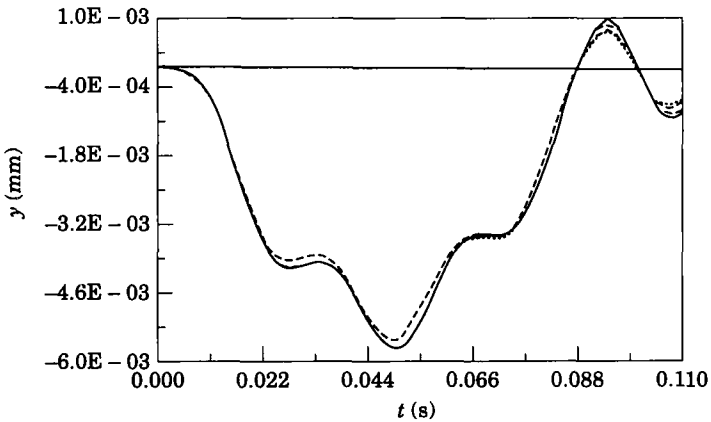


Figure 8. The time history diagram at the middle, for thick beam data. Key as Figure 7.

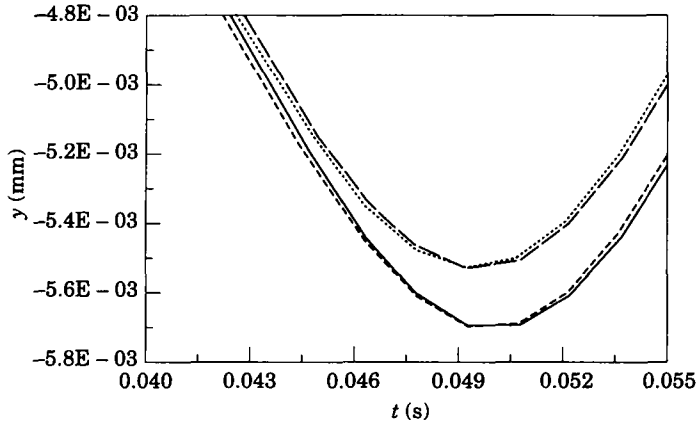


Figure 9. Part of the time history diagram shown in Figure 8. Key as Figure 7.

Clearly, if both the shear deformation and rotary inertia are to be neglected (resulting in the formulation for the Euler–Bernoulli beam), then a combination of the foregoing formulations should be utilized.

5. ALGORITHM OF SOLUTION

For any boundary conditions, two components of  $q_1$  and  $q_N$  are known at all times. For instance, in the case of a simply supported beam,

$$M_1 = M_N = 0, \quad z_1 = z_N = 0. \tag{42}$$

Therefore, if  $q_1$  can be related to  $q_N$ , a set of four equations with four unknowns would be generated.

By using equation (37) it may be simply verified that

$$q_1 = M_{N-1}q_N + T_{N-1}, \tag{43}$$

where  $M_{N-1} = A_1A_2 \cdots A_{N-1}$ ,  $T_{N-1} = B_1 + A_1B_2 + A_1A_2B_3 + \cdots + A_1A_2 \cdots A_{N-2}B_{N-1}$ ,  $A_i = -C_i^{-1}D_i$  and  $B_i = C_i^{-1}E_i$ . Equation (43) can now be solved for  $S_1^+$ ,  $Q_1^+$ ,  $S_N^+$  and  $Q_N^+$ . Hence,  $q_1$  and  $q_N$  are computed. After having calculated  $q_1$  and  $q_N$ , all other  $q_i$  may be evaluated through implementation of equation (37), with  $q_N$  as input. The value of  $q_1$

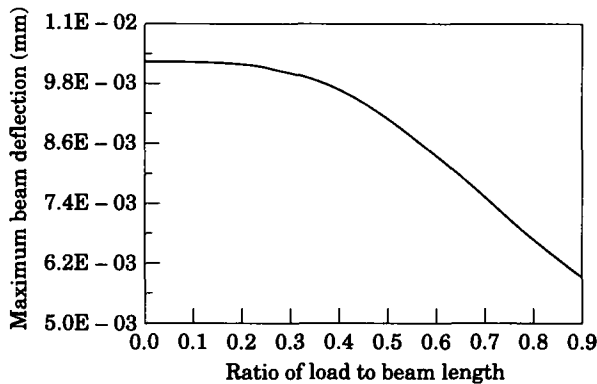


Figure 10. Variation of the maximum beam deflection with the load distribution length.

obtained through this back substitution process can be compared with the one obtained by using equation (43), and the difference is a measure of the computational error. After completing this process,  $E_i$ , used for computations of the next time interval, is calculated and the solution continues.

Finally, since the algorithm gives  $z_i$  values at each time step, for calculation of deflection results standard numerical integration methods are implemented.

## 6. NUMERICAL EXAMPLE

As a numerical example, the above algorithm has been run for the data considered in reference [7], in which the point mass case was considered, and the effects of shear deformation and rotary inertia of the beam were neglected. However, for the present analysis these effects are taken into consideration. The parameters of the problem are as follows:  $L = 4.352$  m,  $E = 2.02 \times 10^{11}$  N/m<sup>2</sup>,  $G = 7.7 \times 10^{10}$  N/m<sup>2</sup>,  $I = 5.71 \times 10^{-7}$  m<sup>4</sup>,  $\rho = 15\,267$  kg/m<sup>3</sup>,  $R = 0.1$ ,  $A = 1.31 \times 10^{-3}$  m<sup>2</sup>,  $M_p = 21.8$  kg,  $V = 27.49$  m/s,  $k = 0.7$ ,  $N = 61$ ,  $\gamma = 10$  and  $g = 9.806$  m/s<sup>2</sup>.

It was observed that for very fine meshes which can model the beam as a continuous system (a large value of  $N$ ), the computational error increases as a result of too many calculations. The error also increases for coarse mesh selections (small  $N$ ), due to poor simulation of the continuous system. The optimal mesh is dependent upon the specific problem under consideration and the authors have no general recommendations about it.

In Figures 2 and 3 are demonstrated, respectively, the time history diagram for the center point of the beam, and the trajectory of the moving mass center for the above data. The beam deflected shape at  $t = 0.1$  s is represented in Figure 4. As can be observed in Figure 2, when using the present method, the maximum beam deflection is found to be about 5.78 mm. However, the corresponding value as quoted in reference [7] is 5.84 mm, and the maximum static deflection of the beam under consideration is about 3.11 mm. Furthermore, the authors have reported [12] that the maximum beam deflection has been evaluated to be 5.73 mm.

The values of maximum dynamic bending moments and shearing forces generated in the beam are very important when designing the load-carrying beams. The respective variations of the maximum bending moment and shearing force (positive or negative) induced in the beam with respect to time are illustrated in Figures 5 and 6. As is seen, the peak values for these parameters occur almost simultaneously, which is critical from a designer's point of view. Furthermore, it should be noted that these figures are not the time history diagrams for the corresponding quantities at a certain point of the beam. They represent the maximum values of bending moment and shear force induced at points along the beam and each instant of time.

The foregoing problem was also solved for cases in which one or both of the parameters, shear deformation and rotary inertia are neglected. Part of the time history diagram for the center of the beam corresponding to the four cases of a Timoshenko beam, a Rayleigh beam, a shear beam and an Euler-Bernoulli beam, with the same data as before, is presented in Figure 7. It is observed that the Timoshenko beam assumptions correspond to some higher maximum beam deflection value. However, for the present problem, this difference is quite slight and is limited to 0.1%. The slightness of this value is predictable, since the beam data introduced is for a thin beam. Hence, it may be concluded that the Euler-Bernoulli beam assumption suffices for this case.

For the case of a thick beam, the following parameters were considered:  $L = 4.352$  m,  $E = 2.02 \times 10^{11}$  N/m<sup>2</sup>,  $G = 7.7 \times 10^{10}$  N/m<sup>2</sup>,  $I = 3.42 \times 10^{-3}$  m<sup>4</sup>,  $\rho = 15\,267$  kg/m<sup>3</sup>,

$R = 2 \times 10^{-4}$ ,  $A = 0.2025 \text{ m}^2$ ,  $M_p = 200 \text{ kg}$ ,  $V = 50 \text{ m/s}$ ,  $k = 0.85$ ,  $N = 61$ ,  $\gamma = 6$  and  $g = 9.806 \text{ m/s}^2$ .

The time history diagrams for the response of the center point of the thick beam are presented in Figures 8 and 9. It was observed that for this thick beam data the maximum difference between the responses obtained corresponding to Timoshenko and Euler–Bernoulli beam assumptions is about 3.6%. Furthermore, as could be deduced from Figures 7 and 9, the effect of shear deformation is much more than that of the rotary inertia.

The variation of the maximum dynamic deflection of the beam with the variation of  $\varepsilon/L$  is presented in Figure 10. When performing this analysis, a system with the thick beam data was considered. As is seen, increasing  $\varepsilon/L$  always results in decreasing the maximum beam deflection. This can be understood as a result of decreasing the time interval in which the dynamic force is exerted, and the time during which all of the load is on the beam.

## 7. CONCLUSIONS

The dynamic behavior of a Timoshenko beam carrying a partially distributed moving mass has been analyzed. The non-dimensionalized equations of motion were transformed into equivalent finite difference ones, and then solved. Results have been presented not only for the deflection, but also for the slope, shearing force and bending moment for all instants of time and at selected space nodes. Hence, all the components composing the dynamic response of the system have been obtained. The procedure has imposed no restricting assumptions on the boundary conditions of the beam. The computations and results for the case of simply supported beams are found to be in good agreement with those obtained for the special case of negligible shear deformation and rotary inertia, and with a short length of load distribution. As a continuation, the system response has been obtained by ignoring either the rotary inertia or the shear deformation, or both of them. It was observed that the effect of shear deformation is usually more important than that of rotary inertia. Furthermore, the total influence of these factors was observed to be about 3.6%, and these effects are in the direction of increasing the maximum beam deflection. As a concluding remark, it was observed that by increasing the length of the load distribution (while conserving the total amount of the load) a decrease in the maximum dynamic deflection of the beam is obtained which is essentially the result of a decrease in the time during which the total load acts on the beam.

## REFERENCES

1. G. G. STOKES 1849 *Transactions of the Cambridge Philosophical Society* **8**, 707–735. Discussion of a differential equation relating to the breaking of railway bridges.
2. S. TIMOSHENKO 1927 *Transactions of the American Society of Mechanical Engineers* **49–50**, 53–61. Vibration of bridges.
3. C. E. INGLIS 1934 *A Mathematical Treatise on Vibration in Railway Bridges*. Cambridge: Cambridge University Press.
4. S. TIMOSHENKO, D. H. YOUNG and W. WEAVER 1974 *Vibration Problems in Engineering*. New York: John Wiley; fourth edition.
5. M. M. STANISIC and J. C. HARDIN 1969 *Journal of The Franklin Institute* **287**, 115–123. On the response of beams to an arbitrary number of concentrated moving masses.
6. C. M. LEECH and B. TABARROK 1970 *Proceedings of the Symposium on Structural Dynamics* **2**, 1–27. The Timoshenko beam under the influence of a travelling mass.
7. A. O. CIFUENTES 1989 *Finite Elements in Analysis and Design* **5**, 237–246. Dynamic response of a beam excited by a moving mass.

8. L. FRÝBA 1972 *Vibration of Solids and Structures Under Moving Loads*. Groningen: Noordhoff.
9. M. GHORASHI 1994 *Ph.D. dissertation, Sharif University of Technology, Tehran*. Dynamic and vibratory analysis of beams under dynamic loads induced by travelling masses and vehicles.
10. E. ESMAILZADEH and M. GHORASHI 1995 *Journal of Engineering* **8**, 213–220. Vibration analysis of beams traversed by a moving mass.
11. M. GHORASHI and E. ESMAILZADEH 1993 *Proceedings of the Second Canadian International Composites Conference*, 749–756. Induced oscillation of beams subjected to dynamic loadings.
12. E. ESMAILZADEH and M. GHORASHI 1995 *Journal of Sound and Vibration* **184**, 9–17. Vibration analysis of beams traversed by uniform partially distributed moving masses.
13. Y.-H. LIN 1996 *Personal communications*. Comments on “Vibration analysis of beams traversed by uniform partially distributed moving masses”. See also Y.-H. LIN 1996 *Journal of Sound and Vibration* **199**, 697–700.
14. H. P. LEE 1994 *Journal of Sound and Vibration* **171**, 361–368. Dynamic response of a beam with intermediate point constraints subject to a moving load.
15. R. F. KELTIE and C. C. CHENG 1995 *Journal of Sound and Vibration* **187**, 213–228. Vibration reduction of a mass-loaded beam.
16. J. J. KALKER 1996 *Vehicle System Dynamics* **25**, 71–88. Discretely supported rails subjected to transient loads.
17. J. S. WU, M. L. LEE and T. S. LAI 1987 *International Journal for Numerical Methods in Engineering* **24**, 743–762. The dynamic analysis of a flat plate under a moving load by the finite element method.
18. A. CIFUENTES and S. LALAPET 1992 *Computers and Structures* **42**, 31–36. A general method to determine the dynamic response of a plate to a moving mass.

#### APPENDIX: AUTHORS' REPLY TO Y.-H. LIN [13]

The authors would like to express their thanks to Professor Y.-H. Lin [13] for his comments on the previous paper [12]. It should be emphasized that the basic idea in reference [12] was to introduce and formulate the moving mass problem when the length of the distributed load distribution is not too small compared with the beam. The beam is assumed to be the Euler–Bernoulli one, with partial (not the total) derivative formulation for the load acceleration. Furthermore, only the interval in which all of the load is on the beam has been considered. Much of the foregoing simplifications have been relaxed and detailed solutions have been presented in reference [9] and in the present paper. These include solutions for motion of distributed loads on Timoshenko beam, using total derivative formulation for the load acceleration, and consideration of the motion not only when all of the load is on the beam, but also during the load entrance, departure and, finally, for the free vibrations. The comments given in reference [13], with the corresponding replies, are summarized as follows.

1. “*Use of the Euler–Bernoulli equation is inappropriate . . .*”. It is evident that the application of complete formulations for the beam response may lead to a more accurate result, as presented here. However, the simple Euler–Bernoulli formulation has been used by many investigators (see, e.g., references [14–16]). While this formulation restricts the domain of application, it can well be used in calculating the system response relatively accurately.

2. “*Total derivative formulation, instead of the partial derivative one is expected for proper expression of the moving mass acceleration . . .*”. While for high speeds these formulations result in different values, at relatively low speeds the difference is of practically no importance. Therefore, in many papers (see, e.g., references [15, 17, 18]), the partial derivative formulation has been utilized, accordingly. However, in reference [9] and the present paper, the total derivative formulation has been used in order to find an accurate solution for the high load speeds.

3. “*The presented procedure in reference [12] needs to be modified in order to be applicable for beams with boundary conditions other than that of simply supported . . .*”. Equation (5) in reference [12] gives the beam deflection function in terms of normalized deflection curves for each mode of the vibrating beam. These can be computed through solution of the free vibration problem. Hence, after solving equation (9) in reference [12], by substituting the result in equation (5), the solution for the beam response, for arbitrary boundary conditions, may essentially be obtained.